Article

The cyclopropane ring as a reporter of radical leaving-group reactivity for Ni-catalyzed C(sp3)–O arylation

L. Reginald Mills, John Monteith, Gabriel dos Passos Gomes, Alan Aspuru-Guzik, and Sophie A.L. Rousseaux

J. Am. Chem. Soc., **Just Accepted Manuscript** • DOI: 10.1021/jacs.0c06904 • Publication Date (Web): 01 Jul 2020

The cyclopropane ring as a reporter of radical leaving-group reactivity for Ni-catalyzed C(sp^3)–O arylation

L. Reginald Mills,[1] John J. Monteith,[1] Gabriel dos Passos Gomes,[1,2] Alán Aspuru-Guzik,[1,2,3,4] and Sophie A. L. Rousseaux[1,*]

[1] Department of Chemistry, University of Toronto, 80 St. George Street, Toronto, ON M5S 3H6, Canada
[2] Department of Computer Science, University of Toronto, 214 College St., Toronto, Ontario M5T 3A1, Canada
[3] Vector Institute for Artificial Intelligence, 661 University Ave. Suite 710, Toronto, Ontario M5G 1M1, Canada
[4] Lebovic Fellow, Canadian Institute for Advanced Research (CIFAR), 661 University Ave, Toronto, ON M5G 1M1, Canada

ABSTRACT: The ability to understand and predict reactivity is essential for the development of new reactions. In the context of Ni-catalyzed C(sp^3)–O functionalization, we have developed a unique strategy employing activated cyclopropanols to aid the design and optimization of a redox-active leaving group for C(sp^3)–O arylation. In this chemistry, the cyclopropane ring acts as a reporter of leaving-group reactivity, since the ring-opened product is obtained under polar (2e) conditions, and the ring-closed product is obtained under radical (1e) conditions. Mechanistic studies demonstrate that the optimal leaving group is redox-active and are consistent with a Ni(I)/Ni(III) catalytic cycle. The optimized reaction conditions are also used to synthesize a number of arylcyclopropanes, which are valuable pharmaceutical motifs.

Introduction

The design of cross-coupling reactions that enable functionalization of new coupling handles that are present in readily available building blocks is of high value since these tools enable more facile access to important molecular motifs, especially those prominent in valuable classes of compounds like pharmaceuticals and agrochemicals. One significant development in the area of Ni catalysis is the use of relatively inert C(sp^2)–O and C(sp^3)–O bonds as coupling partners, which are derived from simple alcohols.[1] While this strategy has been widely explored, the overwhelming reactivity regime for the functionalization of these substrates follows a Ni(0)/Ni(II) catalytic cycle, which does not utilize the unique redox-activity and oxidation states of Ni.[2] To date, there are very few examples of redox-active leaving groups which have been directly functionalized by Ni without the aid of an external photocatalyst or reductant.[3–5] Protocols employing redox-active alcohol derivatives possess the advantages of radical chemistry, namely being able to functionalize activated alcohols without the mechanistic limitations of two-electron (S_N1- and S_N2-type) substitution, and the general ability to perform cross-coupling reactions under relatively mild conditions.[2b] Ultimately, more general strategies which employ redox-active C(sp^3)–O leaving groups in Ni catalysis may aid the rational design of future coupling partners.

The ability to understand the factors that govern reactivity and selectivity for specific reaction pathways is crucial to efficient reaction development. In line with our group's interest in the chemistry of cyclopropanol functionalization[6] and related Ni-catalyzed transformations,[7] we envisioned a unique strategy for the C(sp^3)–O arylation of cyclopropanols, which may aid in the understanding and design of redox-active partners for Ni-catalyzed cross-coupling. Namely, cyclopropyl electrophiles reveal two-electron versus one-electron reactivity via the product obtained in a substitution reaction (Figure 1). When cyclopropyl electrophiles are treated to two-electron substitution chemistry, the ring-opened product is typically obtained; concerted substitutions result in an S_N2' pathway (Figure 1a, top arrow),[8] while S_N1 reactions occur via rapid ring-opening of the cyclopropyl cation[9] (Figure 1a, bottom arrow).[10,11] Alternatively, cyclopropyl radicals have a lifetime which allows them to be captured without rupture of the cyclopropane.[12] Thus, the one-electron substitution process can retain the cyclopropane ring. In the context of

Ni catalysis, a number of redox-active leaving groups have been employed for cyclopropane functionalization, including iodides,[13] bromides,[14] *N*-hydroxyphthalimide esters (derived from carboxylic acids),[15] and pyridinium salts (derived from cyclopropylamines) (Figure 1b).[16–18]

Figure 1. Polar and radical cyclopropane reactivity

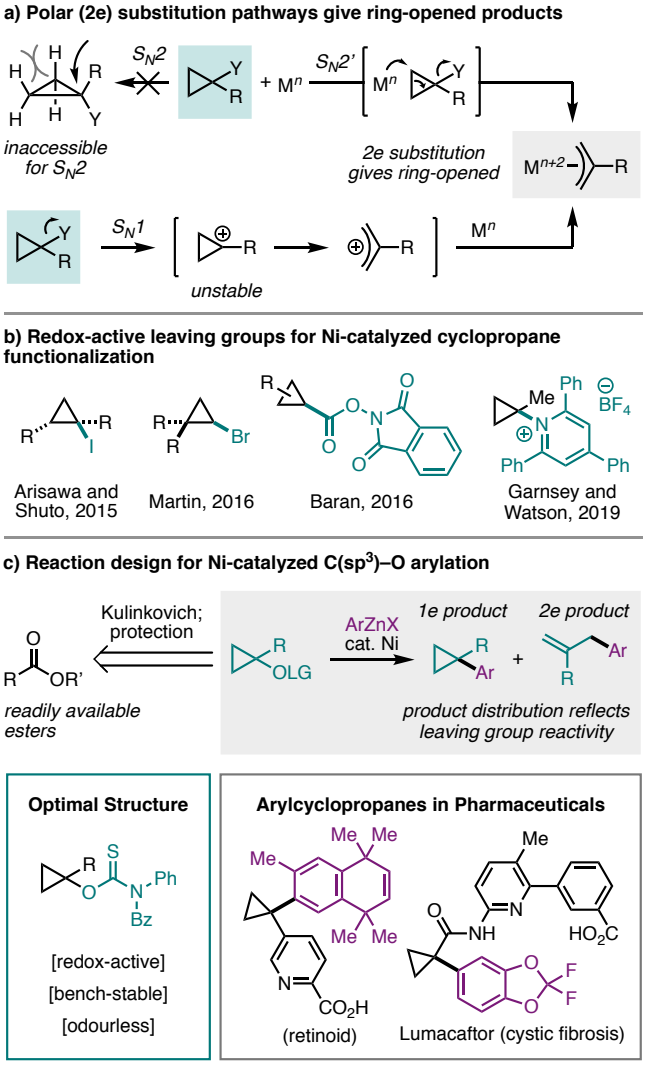

For the Ni-catalyzed C(sp^3)–O functionalization reaction of cyclopropanols, the product distribution would directly reflect the reactivity of the leaving group (Figure 1c, right arrow), with the arylcyclopropane product being obtained from a redox-active leaving group. In this sense, the cyclopropane itself acts as a reporter of two- versus one-electron reactivity and enables optimization for desired reactivity. Using this scheme, we discovered that an *N*-benzoyl carbamothioate derivative is an optimal leaving-group structure for C(sp^3)–O arylation of cyclopropanols (Figure 1c, bottom left box). These redox-active starting materials are bench-stable, odorless, and prepared in one step from readily available cyclopropanols (Figure 1, retrosynthesis arrow).[19] Further, the arylation of these starting materials provides access to desirable arylcyclopropane derivatives, which are important motifs in pharmaceuticals[20–22] (Figure 1c, bottom right box).

Results and Discussion

We began exploring the reactivity of activated cyclopropanols under Ni-catalyzed Negishi-type conditions (Table 1), employing an arylzinc reagent (3 equiv) (prepared from the corresponding Grignard reagent[23]), Ni source (10 mol %), and ligand, in 1,4-dioxane/THF at 23 or 110 ºC for 12 h. A heat-map representation is employed to demonstrate the leaving group's propensity to undergo polar (2e) reactivity with formation of ring-opened product **2a** (red) or radical (1e) reactivity with formation of ring-intact isomer **3a** (green). It should be noted that the optimal conditions for polar and

Figure 2. Optimization of the leaving group[a]

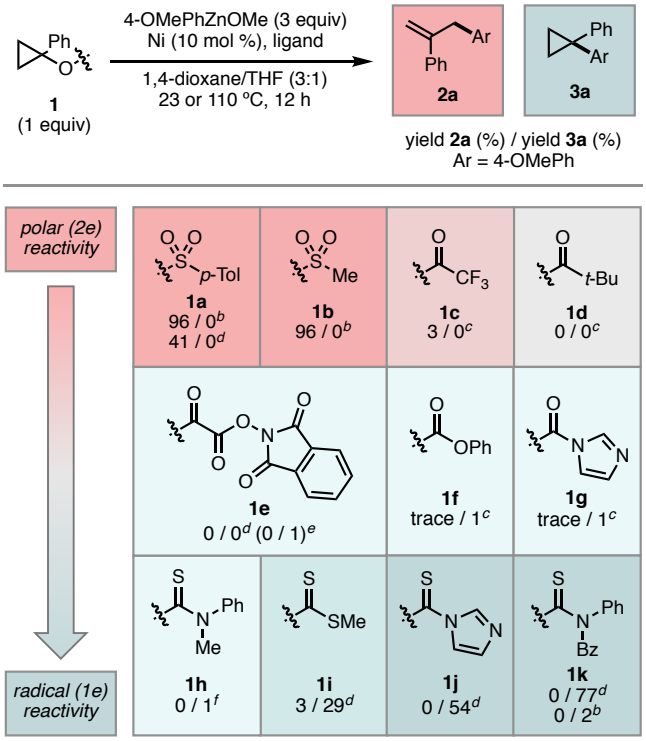

[a]Reactions performed on 0.10-mmol scale. Yields determined by GC-MS using *n*-dodecane as internal standard. For full details, see SI (Table S1); [b]Using $NiCl_2(PPh_3)_2$ at 110 ºC; [c]Using $NiCl_2(PCy_3)_2$ at 110 ºC; [d]Using $Ni(acac)_2$•xH_2O and bathocuproine (20 mol %) at 23 ºC; [e]Using $NiCl_2$(dme), dtbbpy (20 mol %), $Ru(bpy)_3(PF_6)_2$ (1 mol %), blue LEDs, ArZnCl (2 equiv) and acetone/THF (1:1); [f]Using $NiCl_2$(dme) and neocuproine (20 mol %) at 23 ºC.

radical reactivity differ in terms of the Ni source, ligand, and reaction temperature. Thus, for simplicity, Figure 2 explores the trend in reactivity according to conditions that best represent a leaving group's reactivity (see SI for full details). Cyclopropyl tosylate **1a**, which is known to undergo S_N2'-type and S_N1 reactions,[8,10a] selectively yielded the ring-opened product using $NiCl_2(PPh_3)_2$ at 110 ºC.[24] Under the same conditions, mesylate **1b** also selectively gave the ring-opened isomer. Less labile leaving groups, esters **1c** and **1d**, were largely unreactive under the reaction conditions, however, **2a** could be obtained in trace amounts from **1c** using $NiCl_2(PCy_3)_2$ at 110 ºC. The first evidence that a redox-active leaving group could deliver the desired arylated cyclopropane product was obtained with *N*-hydroxyphthalimide oxalate **1e**.[25,4a] While **1e** was unproductive in the presence of Ni alone, **3a** was obtained in 1% yield in the presence of photocatalyst $Ru(bpy)_3(PF_6)_2$ and blue LEDs. No ring-opened isomer **2a** was detected in this case. Phenyl carbonate **1f**, as well as imidazole carbamate derivative **1g**, each yielded trace amounts of **3a**, however, **2a** was also detected in both cases. Based on our hypothesis that a radical-based strategy could afford the desired cyclopropane product, we probed redox-active leaving groups used in Barton–McCombie deoxygenation reactions.[26] Using $NiCl_2$(dme) and neocuproine at 23 ºC, *N*-methyl thiocarbamate **1h** delivered cyclopropane **3a** in 1% yield with no detectable amount of **2a**. Xanthate **1i** and thiocarbonyl imidazolide **1j** both delivered **3a** in moderate yield and good selectivity using Ni(acac)$_2$•xH_2O and bathocuproine. Finally, *N*-benzoyl carbamothioate **1k** gave the desired cyclopropane in high yield and excellent selectivity. With the exception of **1e**, the reaction mass balance with low-yielding substrates was unreacted starting material. Notably, the preference for polar vs. radical reactivity in Figure 2 can be attributed to the nature of the leaving group, since the reactions of **1a** and **1k** under the opposite group's optimal ligand set and conditions (bathocuproine and PPh_3, respectively) still gave the same product selectivity, albeit in much lower yields.

Under the optimized reaction conditions using substrate **1k**, the major side-product is thioester **4a** (Figure 3a). Thioester **4a** is not observed in the absence of Ni (Figure 3a, third entry), and the formation of both **3a** and **4a** shows a significant ligand dependence (Table S2). The yield of **4a** can also be increased by changing the reaction solvent (Figure 3a, second entry). Thioester **4** likely arises from the recombination of a Ni–aryl species with an alkoxythiocarbonyl radical (**5**),[26b] followed by reductive elimination. Alkoxythiocarbonyl radical **5** is a well-established intermediate in Barton–McCombie chemistry.[27,28] Further, while leaving group **1k** has not been previously reported for Barton–McCombie deoxygenation, it readily participates in this reaction, indicating that **1k** is redox-active; in our hands, the deoxygenated product was obtained in 65% yield, as determined by ^{1}H NMR (Equation S1).

It is known that thioesters such as **4** are redox-active and can participate in Barton–McCombie deoxygenations.[26a] Thus, we were interested in seeing if **4a** could act as an active coupling partner under our reaction conditions (Figure 3b). When **4a** was exposed to standard reaction conditions, full conversion was observed, with 82% of **3a** being formed, as determined by GC-MS (Figure 3b). These results demonstrate that **4** is catalytically competent, and strongly suggests its role as an intermediate on route to the formation of **3a**.

Figure 3. Thioester reactivity

a) Formation of thioester side-product[a]

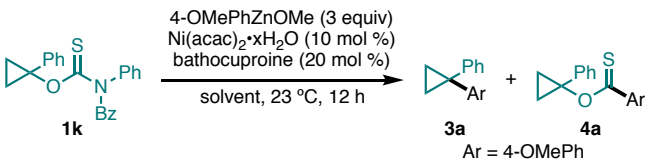

solvent	yield **3a** (%)	yield **4a** (%)
1,4-dioxane/THF (3:1)	78	12
THF	1	66
1,4-dioxane/THF (2:1)[b]	0	0

via: **5**

b) Catalytic competence of 4a

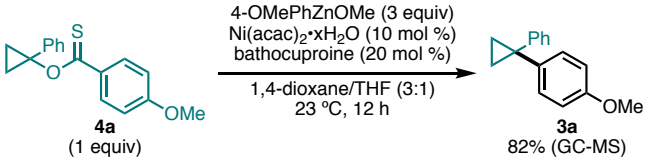

[a]See SI for details; [b]Without Ni.

Together, these results suggested that a dual catalytic cycle was operable under the reaction conditions, with one Ni(I)/Ni(III) catalytic for the conversion of thiocarbamate **1** to thioester **4**, and another for the conversion of **4** to arylcyclopropane **3**. In the first catalytic cycle, Ni(I)–X intermediate **6** can undergo transmetallation to form Ni(I)–aryl intermediate **7**. Single-electron transfer from **7** to thiocarbamate **1** will give radical anion **9** and Ni(II)–aryl cation **8**. Fragmentation of **9** will yield thioacyl radical **5**.[27] Recombination of **5** with **8** will form Ni(III) intermediate **10**, which can undergo reductive elimination to release thioester **4** and regenerate Ni(I)–X intermediate **6**. In the second catalytic cycle, Ni(I)–aryl intermediate **7** can perform single-electron transfer with **4** to form radical anion **11** and Ni(II)–aryl cation **8**. Fragmentation of radical anion **11** can generate

Figure 4. Proposed reaction mechanism

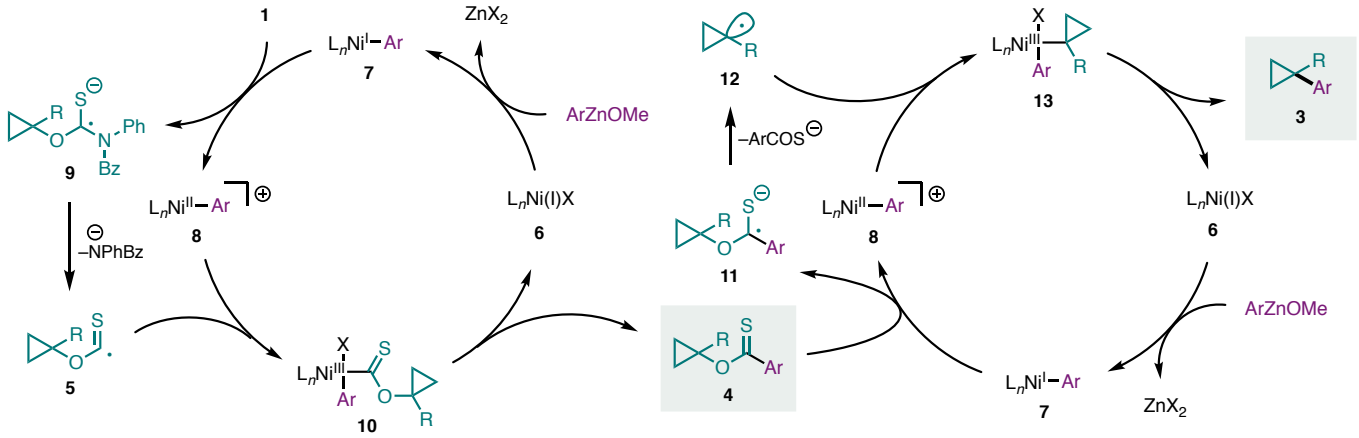

cyclopropyl radical **12**, which will quickly recombine with **8** to form Ni(III) species **13**. Then, reductive elimination will form arylcyclopropane **3** and regenerate Ni(I)–X intermediate **6**. Based on our mechanistic studies (Figure 5), it is likely that the radical anions and Ni(II) cations (**9** and **8**; and **11** and **8**) are solvent-caged contact-ion pairs.

Under catalytic conditions, we also noticed a correlation between the yield of thioester side-product **4** and the electronic properties of the arylzinc reagent (Figure 5a).[29] While the use of the 4-methoxyphenylzinc reagent results in good yield of cyclopropane (**3a**) and only 12% yield of the thioester (**4a**) (entry 1), using the 4-fluorophenylzinc reagent results in a more significant 54% yield of the thioester (**4b**). This suggests that the thioester (**4**) is efficiently formed in both cases, but that the OMe-substituted thioester more readily goes on to form cyclopropane. To support this catalytic scenario, we performed crossover experiments between 4-methoxyphenyl thioester **4a** and 4-fluorophenylzinc chloride, as well as between 4-fluorophenyl thioester **4b** and 4-methoxyphenylzinc chloride (Figure 5b). Under standard reaction conditions, **4a** gave the desired product **3b** in 49% yield,[30] with no detectable formation of 4-methoxyphenyl cyclopropane (**3a**), as determined by GC-MS. Alternatively, the crossover experiment with 4-fluorophenyl thioester **4b** gave only a 5% yield of desired product **3a**, with no detectable formation of 4-fluorophenyl cyclopropane (**3b**). These results indicate that the 4-methoxyphenyl thiobenzoate substituent is a competent leaving group and that the arene found in product **3** comes from a second equivalent of arylzinc reagent (cf. Table S5).

This difference in reactivity between electron-rich and -deficient thiobenzoates was intriguing since we reasoned that fragmentation radical anion (**11**) should be facilitated by a more electron-withdrawing substituent that would stabilize the anionic intermediate and promote conversion of the thiobenzoate ester. Yet, this was at odds with the preference of the apparently more electron-rich 4-methoxyphenyl thiobenzoate (**4a**) to undergo conversion to cyclopropane (**3a**). To gain a better understanding of this mechanism, the kinetics for fragmentation of a radical anion (**11**) to form a cyclopropyl radical (**12**) and a thiobenzoate anion (**14**) were studied computationally, for derivatives with either a 4-fluorophenyl (X = F, **11b**) or 4-methoxyphenyl (X = OMe, **11a**) substituent on the thiobenzoate (Figure 6). When the transition state

Figure 5. Reactivity of *para*-substituted (a) arylzinc reagents and (b) thioesters with arylzinc reagents

a) Formation of cyclopropane 3 vs. thioester 4 as a function of the electronic properties of the *para*-substituted arylzinc reagent

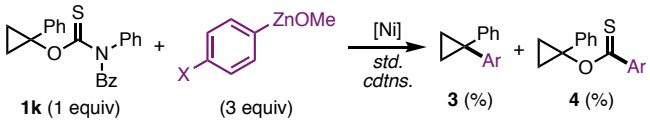

Entry	X	Yield **3** (GC-MS)	Yield **4** (GC-MS)
1	OMe (**a**)	78%	12%
2	F (**b**)	10%	54%

b) Arylzinc crossover experiments

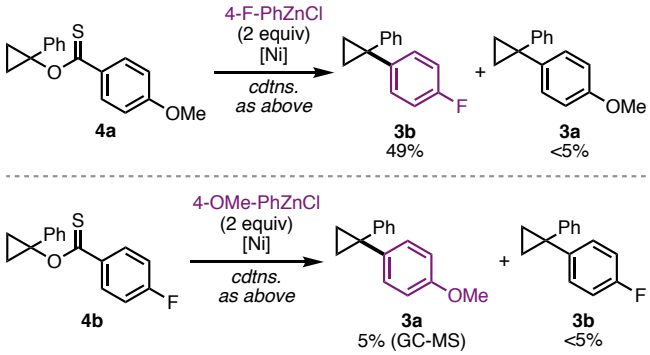

energies for fragmentation were compared, the barrier for fragmentation of the radical anion with a 4-methoxy substituent (X = OMe, **11a**) was 2.1 kcal/mol lower than that for fragmentation of the 4-fluoro derivatives (X = F, **11b**), consistent with experimental observations (Figure 5). This energy difference can be attributed to a key stabilizing effect

of the O–CH_3 antibonding orbital, which can accept negative charge from the aromatic system via hyperconjugation[31] ($\pi_{CC} \rightarrow \sigma^*_{CO}$ = 2.3 kcal/mol).[32] This can be observed in the calculated geometry of the OMe group (Figure 6, top right structure) does not lie in plane, the usual geometry where the *p*-type lone pair overlaps with the aromatic π-system. Rather, the OMe group adopts an orthogonal geometry to enable overlap of the O–CH_3 antibonding orbital with the π-system. Thus, in this case, the OMe group acts not as an electron-donating group, but as a charge-stabilizing substituent, resulting in a lower barrier for fragmentation when compared to the F group. The chameleonic nature of methoxy substituents in the stabilization of negative charge has been previously documented.[33,34]

Figure 6. Kinetic profile for fragmentation of radical anion **6**. Level of theory: (SMD=1,4-dioxane)/UωB97X-D2/6-311++G(2d,p)

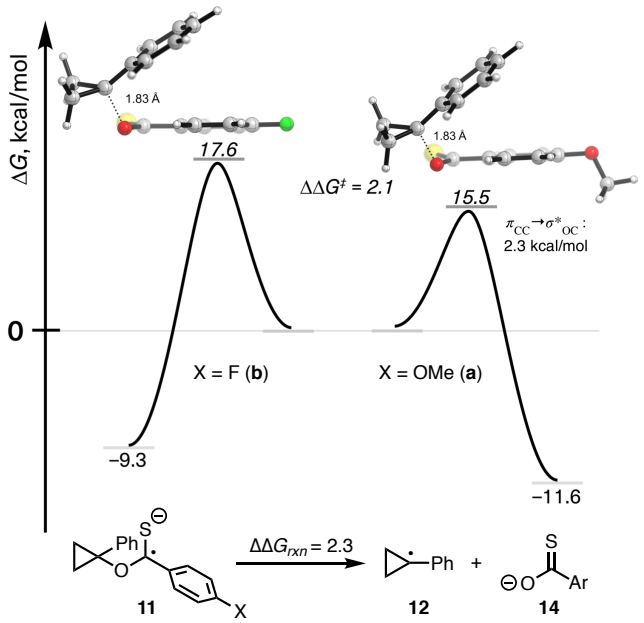

With this data in hand, experiments were performed to validate the role of radical intermediates. First, enantioenriched thiocarbamate substrate **15** was exposed to standard reaction conditions, and product **16** was obtained as a racemic mixture (Figure 7a). This is consistent with fragmentation to generate a benzylic radical.[35] We also submitted diastereomers *cis*-**17**, *cis*-**18**, and *trans*-**17** to the standard reaction conditions (Figure 7b). All of these reactions yielded the arylated cyclopropane with complete diastereospecificity, and no detection of the opposite stereoisomer. It is known that cyclopropyl radicals have a barrier to inversion, and that stereochemistry is maintained in cases of radical disproportionation[36] and in solvent-caged recombination with transition metal catalysts.[37,38] Namely, for solvent-caged cyclopropyl radicals, it has been estimated by Walborsky that the rate of reaction within the solvent cage is faster than the rate of inversion, and that the configuration of the cyclopropane should remain largely intact.[12] For this reaction, the in-cage reaction would be recombination of the Ni(II)–cyclopropyl radical pair to form a Ni(III) intermediate (Figure 7b, right bracket).[39–41] The remaining mass balance in these reactions is the thioester intermediate (**4**). While the yields for the reactions using these multisubstituted cyclopropanes are lower than those for 1-arylcyclopropanes, increased conversion to the product can be achieved using higher catalyst loading (20 mol %) and 4 equiv of arylzinc reagent (*trans*-**17**, 28%).

Figure 7. Stereochemical outcome of the reaction

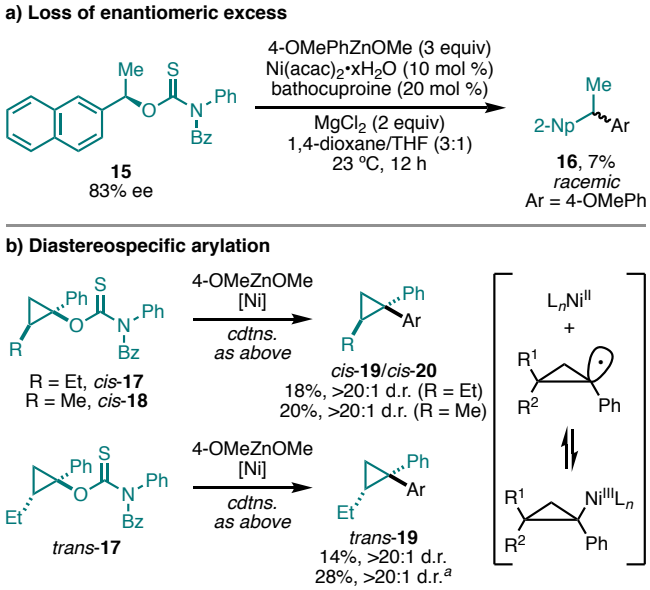

[a]Using 20 mol % Ni and 4 equiv 4-OMeZnOMe.

Finally, we explored the scope of cyclopropanes accessible under the optimized conditions (Table 1).[42] Electron-rich (**3c**–**3e**) and electron-deficient (**3f**, **3g**) cyclopropanols are compatible substrates. Radical-stabilizing π-susbtituents (**3h**, **3i**) work efficiently. Bicyclic cyclopropanes (**3j**–**3l**) can also be accessed in moderate yields. While alkyl-substituted cyclopropanols are less efficient substrates, conversion to the desired product can be improved using greater amounts of arylzinc reagent and higher catalyst loading (**3m**).

With respect to the arylzinc reagent, alkoxy- and amino-substituted arenes (**3n**–**3p**) can be employed, as well as heteroaromatic arenes (**3q**–**3s**). For incompatible arylzinc reagents, the major product is thioester **4**, and poor conversion to cyclopropane is achieved (see Table S8).[43] We hypothesize that viable arylzinc reagents have some charge-stabilizing property which assists with fragmentation (Figure 6). For electron-neutral (hetero)arylzinc reagents (**3t**–**3w**) that are not viable under standard reaction conditions, the

desired product can be obtained if the 4-methoxyphenyl thioester (**4a**) is used as the redox-active starting material instead.

Table 1. Scope of the reaction[a]

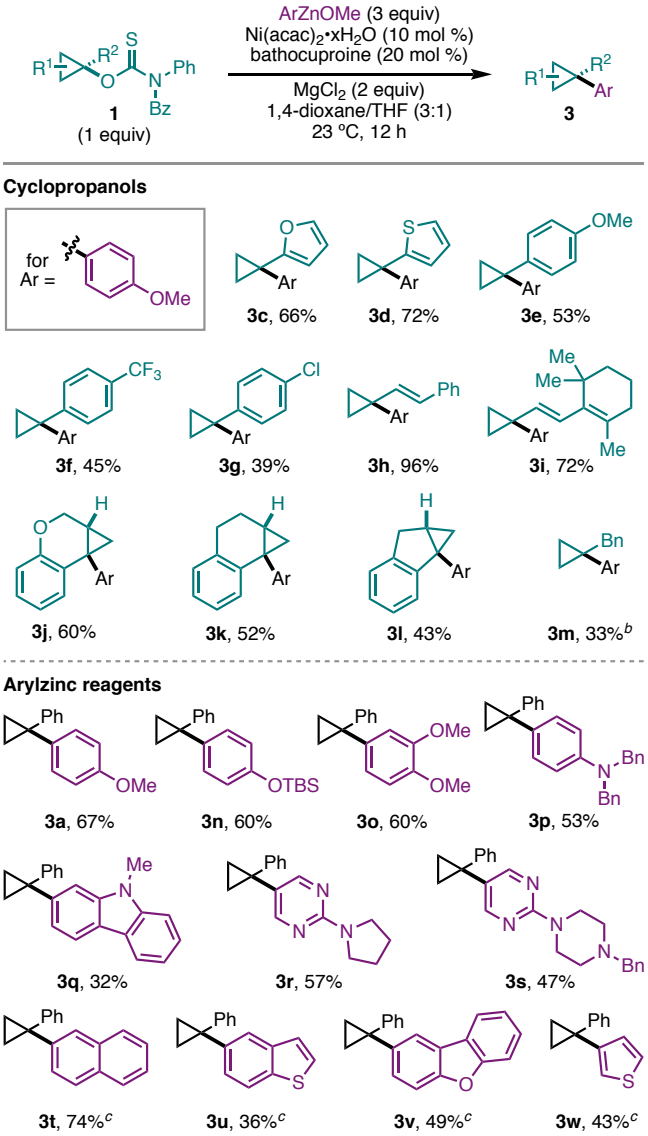

[a]Reactions performed on 0.10–0.40 mmol scale; [b]Using ArZnCl (4 equiv), $Ni(acac)_2•xH_2O$ (20 mol %), and bathocuproine (40 mol %); [c]Using **4a** instead of **1**, ArZnCl (2 equiv), and without $MgCl_2$. For supplementary examples and lower-yielding substrates, see Table S8.

Conclusion

In conclusion, we have discovered a new redox-active leaving group to enable the Ni-catalyzed C(sp^3)–O arylation of cyclopropanols. The discovery of this leaving group was accomplished using a unique optimization strategy in which the redox-activity of the leaving group was reflected in the distribution of ring-closed versus ring-opened products. We believe the optimization strategy used here may aid the prediction of reactivity of activating groups in Ni catalysis, and the development of future cross-coupling reactions. Our results also demonstrate the possibility of extremely short lifetimes for some radicals, sometimes shorter than the time required to activate classical "radical clocks".[39a] Our group is actively exploring Ni-catalyzed functionalization of other alcohol derivatives, using the lessons learned in this chemistry to facilitate leaving group design. We will also soon disclose the scope and mechanistic insights of a Ni-catalyzed ring-opening arylation reaction to form product **2**.

COMPUTATIONAL DETAILS

All DFT calculations were carried out with the *Gaussian 16* software package.[44] Initial geometries were generated with *openbabel*[45] from their SMILES strings, and pre-optimized with Grimme's *xtb 6.2.3*.[46] The initial *xtb*-optimized geometries were used for a thorough conformer search with Grimme's *crest*.[47] Further geometry optimizations were performed with (SMD[48]=1,4-dioxane) for solvation corrections and the unrestricted ωB97X DFT functional[49] employing the 6-311++G(2d,p) basis set for all atoms. Grimme's D2 empirical dispersion corrections[50] were also included. The integration grid emplowed was of 175,974 points for the first-row atoms and of 250,974 points for the atoms in the second and later rows). Frequency calculations were performed to confirm if a structure is a ground or transition state. Paton's *GoodVibes*[51] was used to obtain quasi-harmonic corrections to Gibbs Free Energies (via quasi-harmonic corrections to both entropy and enthalpy, defaulting to the Grimme method for entropy and the Head-Gordon enthalpy correction approach).

Natural Bond Orbital[52] (NBO) analyses were performed with *NBO7* as linked to *Gaussian 16*. They were used to gauge the magnitude of the hyperconjugative interactions in the presented systems. CYLView[53] was used to render the molecules.

ASSOCIATED CONTENT

Reaction optimization tables, mechanistic and stoichiometric studies, synthetic procedures, characterization data, and computational details (PDF)

NMR spectra (PDF)

AUTHOR INFORMATION

Corresponding Author

*E-mail: sophie.rousseaux@utoronto.ca.

ORCID

Sophie A. L. Rousseaux: 0000-0002-6505-5593

L. Reginald Mills: 0000-0002-6329-2368

Gabriel dos Passos Gomes: 0000-0002-8235-5969

Alán Aspuru-Guzik: 0000-0002-8277-4434

Notes

No competing financial interests have been declared.

ACKNOWLEDGMENT

We thank NSERC (Discovery Grants and Canada Research Chair programs), the Canada Foundation for Innovation (Project No. 35261), the Ontario Research Fund, Kennarshore Inc., and the University of Toronto for generous financial support of this work. We also acknowledge the Canada Foundation for Innovation (Project No. 19119) and the Ontario Research Fund for funding the Centre for Spectroscopic Investigation of Complex Organic Molecules and Polymers. L.R.M. thanks NSERC for a graduate scholarship (PGS D). J.J.M. thanks NSERC for a graduate scholarship (CGS M) and the University of Toronto for a doctoral scholarship (FAST). Dr. Jack Sheng (University of Toronto) is thanked for assistance with NMR studies. Nicholas Michel (University of Toronto) is thanked for valuable mechanistic insight. G. P. G gratefully acknowledges NSERC for the Banting Postdoctoral Fellowship. A. A-G. thanks Anders G. Frøseth for his generous support. A. A.-G. also acknowledges the generous support of Natural Resources Canada and the Canada 150 Research Chairs program, Tata Steel, and the Office of Naval Research. We thank *Compute Canada* for computational resources. DFT and NBO computations were performed on the *niagara* supercomputer at the SciNet HPC Consortium. SciNet is funded by: the Canada Foundation for Innovation; the Government of Ontario; Ontario Research Fund - Research Excellence; and the University of Toronto. Dr. Louis-Charles Campeau and Michael S. West are thanked for a critical reading of this manuscript.

REFERENCES

1. (a) Rosen, B. M.; Quasdorf, K. W.; Wilson, D. A.; Zhang, N.; Resmerita, A.-M.; Garg, N. K.; Percec, V. Nickel-Catalyzed Cross-Couplings Involving Carbon-Oxygen Bonds. *Chem. Rev.* **2011**, *111*, 1345–1416; (b) Cornella, J.; Zarate, C.; Martin, R. *Chem. Soc. Rev.* Metal-catalyzed activation of ethers *via* C–O bond cleavage: a new strategy for molecular diversity. **2014**, *43*, 8081–8097; (c) Tobisu, M.; Chatani, N. Cross-Couplings Using Aryl Ethers via C–O Bond Activation Enabled by Nickel Catalysts. *Acc. Chem. Res.* **2015**, *48*, 1717–1726; (d) Tollefson, E. J.; Hanna, L. E.; Jarvo, E. R. Stereospecific Nickel-Catalyzed Cross-Coupling Reactions of Benzylic Ethers and Esters. *Acc. Chem. Res.* **2015**, *48*, 2344–2353.

2. (a) Tasker, S. Z.; Standley, E. A.; Jamison, T. F. Recent advances in homogeneous nickel catalysis. *Nature* **2014**, *509*, 299–309; (b) Fu, G. C. Transition-Metal Catalysis of Nucleophilic Substitution Reactions: A Radical Alternative to S_N1 and S_N2 Processes. *ACS Cent. Sci.* **2017**, *3*, 692–700; (c) Diccianni, J. B.; Diao, T. Mechanisms of Nickel-Catalyzed Cross- Coupling Reactions. *Trends Chem.* **2019**, *1*, 830–844.

3. For a Ni-catalyzed protocol employing aryl carbonates: Oelke, A. J.; Sun, J.; Fu, G. C. Nickel-Catalyzed Enantioselective Cross-Couplings of Racemic Secondary Electrophiles That Bear an Oxygen Leaving Group. *J. Am. Chem. Soc.* **2012**, *134*, 2966–2969.

4. For protocols employing redox-active activating groups for alcohols and Ni catalysis: Oxalate: (a) Zhang, X.; MacMillan, D. W. C. Alcohols as Latent Coupling Fragments for Metallaphotoredox Catalysis: sp^3–sp^2 Cross-Coupling of Oxalates with Aryl Halides. *J. Am. Chem. Soc.* **2016**, *138*, 13862–13865; Xanthate: (b) Vara, B. A.; Patel, N. R.; Molander, G. A. *O*-Benzyl Xanthate Esters under Ni/Photoredox Dual Catalysis: Selective Radical Generation and Csp^3–Csp^2 Cross-Coupling. *ACS Catal.* **2017**, *7*, 3955–3959; Methyl oxalate: (c) Ye, Y.; Chen, H.; Sessler, J. L.; Gong, H. Zn-Mediated Fragmentation of Tertiary Alkyl Oxalates Enabling Formation of Alkylated and Arylated Quaternary Carbon Centers. *J. Am. Chem. Soc.* **2019**, *141*, 820–824.

5. For select protocols employing a redox-active alcohol activating group and transition metal catalysis: (a) Zhu, L.; Liu, S.; Douglas, J. T.; Altman, R. A. Copper-Mediated Deoxygenative Trifluoromethylation of Benzylic Xanthates: Generation of a C–CF_3 Bond from an O-Based Electrophile. *Chem. Eur. J.* **2013**, *19*, 12800–12805; (b) Chenneberg, L.; Baralle, A.; Daniel, M.; Fensterbank, L.; Goddard, J.-P.; Ollivier, C. *Adv. Synth. Catal.* **2014**, *356*, 2756–2762.

6. Mills, L. R.; Barrera Arbelaez, L. M.; Rousseaux, S. A. L. Electrophilic Zinc Homoenolates: Synthesis of Cyclopropylamines from Cyclopropanols and Amines. *J. Am. Chem. Soc.* **2017**, *139*, 11357–11360.

7. Mills, L. R.; Zhou, C.; Fung, E.; Rousseaux, S. A. L. Ni-Catalyzed β-Alkylation of Cyclopropanol-Derived Homoenolates. *Org. Lett.* **2019**, *21*, 8805–8809.

8. Quan, L. G.; Lee, H. G.; Cha, J. K. Acid- and Pd(0)-Catalyzed Ring Opening of 1-(1-Cycloalkenyl)cyclopropyl Sulfonates. *Org. Lett.* **2007**, *9*, 4439–4442.

9. G. Boche, H. M. Walborsky, Cyclopropane Derived Reactive Intermediates (Eds.: S. Patai, Z. Rappoport), Wiley, Chichester, 1990, pp. 117–173.

10. Select examples: (a) DePuy, C. H.; Schnack, L. G.; Hausser, J. W.; Wiedemann, W. Chemistry of Cyclopropanols. III. The Mechanism of the Solvolysis of Cyclopropyl Tosylates. *J. Am. Chem. Soc.* **1965**, *87*, 4006–4006; (b) Hausser, J. W.; Pinkowski, N. J. Solvolysis of cyclopropyl halides. 2-Phenylcyclopropyl chlorides. *J. Am. Chem. Soc.* **1967**, *89*, 6981–6984; (c) Schöllkopf, U. Synthesis of Cyclopropyl Ethers and Cyclopropanols by Carbene Transfer – Acetolysis of Cyclopropyl *p*-Toluenesulfonates. *Angew. Chem. Int. Ed. Engl.* **1968**, *7*, 588–598; (d) von Ragué Schleyer, P.; Su, T. M.; Saunders, M.; Rosenfeld, J. C. Stereochemistry of allyl cations from the isomeric 2,3-dimethylcyclopropyl chlorides. Stereomutations of allyl cations. *J. Am. Chem. Soc.* **1969**, *91*, 5174–5176; (e) Salaün, J. Preparation and substituent effect in the solvolysis of 1-ethynylcyclopropyl tosylates. *J. Org. Chem.* **1976**, *41*, 1237–1240; (f) Kozyrkov, Y. Y.; Kulinkovich, O. G. *Synlett* **2002**, 443–446; Reviews: (g) Sarel, S.; Yovell, J.; Sarel-

Imber, M. Recent Developments in the Stereochemistry of Cyclopropane Ring Opening. *Angew. Chem. Int. Ed. Engl.* **1968**, *7*, 577–588; (h) Kirmse, W.; Schütte, H. Desaminierungsreaktionen, III. Cyclopropyldiazonium-Ionen und Cyclopropylkationen. *Chem. Ber.* **1968**, *101*, 1674–1688; (i) DePuy, C. H. The Chemistry of Cyclopropanols. *Acc. Chem. Res.* **1968**, *1*, 33–41; (j) Gibson, D. H.; DePuy, C. H. Cyclopropanol chemistry. *Chem. Rev.* **1974**, *74*, 605–623; (k) Aksenov, V. S.; Terent'eva, G. A.; Savinykh, Y. V. Nucleophilic Substitution Reactions of Cyclopropane Derivatives. *Russ. Chem. Rev.* **1980**, *49*, 549–557.

11. S_N1 substitution reactions of some cyclopropane derivatives are known: Kozhushkov, S. I.; Späth, T.; Kosa, M.; Apeloig, Y.; Yufit, D. S.; de Meijere A. Relative Stabilities of Spirocyclopropanated Cyclopropyl Cations. *Eur. J. Org. Chem.* **2003**, 4234–4242.

12. Walborsky, H. M. The cyclopropyl radical. *Tetrahedron* **1981**, *37*, 1625–1651.

13. Yotsuji, K.; Hoshiya, N.; Kobayashi, T.; Fukuda, H.; Abe, H.; Arisawa, M.; Shuto, S. Nickel-Catalyzed Suzuki–Miyaura Coupling of a Tertiary Iodocyclopropane with Wide Boronic Acid Substrate Scope: Coupling Reaction Outcome Depends on Radical Species Stability. *Adv. Synth. Catal.* **2015**, *357*, 1022–1028.

14. Moragas, T.; Martin, R. Nickel-Catalyzed Reductive Carboxylation of Cyclopropyl Motifs with Carbon Dioxide. *Synthesis* **2016**, *48*, 2816–2822.

15. (a) Cornella, J.; Edwards, J. T.; Qin, T.; Kawamura, S.; Wang, J.; Pan, C.-M.; Gianatassio, R.; Schmidt, M.; Eastgate, M. D.; Baran, P. S. Practical Ni-Catalyzed Aryl–Alkyl Cross-Coupling of Secondary Redox-Active Esters. *J. Am. Chem. Soc.* **2016**, *138*, 2174–2177; (b) Qin, T.; Malins, L. R.; Edwards, J. T.; Merchant, R. R.; Novak, A. J. E.; Zhong, J. Z.; Mills, R. B.; Yan, M.; Yuan, C.; Eastgate, M. D.; Baran, P. S. Nickel-Catalyzed Barton Decarboxylation and Giese Reactions: A Practical Take on Classic Transforms. *Angew. Chem. Int. Ed.* **2017**, *56*, 260–265; (c) Li, C.; Wang, J.; Barton, L. M.; Yu, S.; Tian, M.; Peters, D. S.; Kumar, M.; Yu, A. W.; Johnson, K. A.; Chatterjee, A. K.; Yan, M.; Baran, P. S. Decarboxylative borylation. *Science* **2017**, *356*, eaam7355; (d) Chen, T.-G.; Barton, L. M.; Lin, Y.; Tsien, J.; Kossler, D.; Bastida, I.; Asai, S.; Bi, C.; Chen, J. S.; Shan, M.; Fang, H.; Fang, F. G.; Choi, H.; Hawkins, L.; Qin, T.; Baran, P. S. Building $C(sp^3)$-rich complexity by combining cycloaddition and C–C cross-coupling reactions. *Nature* **2018**, *560*, 350–354.

16. Liao, J.; Basch, C. H.; Hoerrner, M. E.; Talley, M. R.; Boscoe, B. P.; Tucker, J. W.; Garnsey, M. R.; Watson, M. P. Deaminative Reductive Cross-Electrophile Couplings of Alkylpyridinium Salts and Aryl Bromides. *Org. Lett.* **2019**, *21*, 2941–2946.

17. For a review: Rubin, M.; Rubina, M.; Gevorgyan, V. Transition Metal Chemistry of Cyclopropenes and Cyclopropanes. *Chem. Rev.* **2007**, *107*, 3117–3179.

18. For select transition metal–catalyzed functionalization reactions of cyclopropyl electrophiles: (a) Stolle, A.; Salaün, J.; de Meijere, A. Palladium(0) catalyzed substitution reactions of cyclopropyl group containing allylic esters. *Tetrahedron Lett.* **1990**, *31*, 4593–4596; (b) Stolle, A.; Ollivier, J.; Piras, P. P.; Salaün, J.; de Meijere, A. Nucleophilic substitutions of 1-alkenylcyclopropyl esters and 1-alkynylcyclopropyl chlorides catalyzed by palladium(0). *J. Am. Chem. Soc.* **1992**, *114*, 4051–4067; (c) Charette, A. B.; Giroux, A. Palladium-Catalyzed Suzuki-Type Cross-Couplings of Iodocyclopropanes with Boronic Acids: Synthesis of *trans*-1,2-Dicyclopropyl Alkenes. *J. Org. Chem.* **1996**, *61*, 8718–8719; (d) Charette, A. B.; Pereira De Freitas-Gil, R. Synthesis of contiguous cyclopropanes by palladium-catalyzed Suzuki-type cross-coupling reactions. *Tetrahedron Lett.* **1997**, *38*, 2809–2812; (e) Atlan, V.; Racouchot, S.; Rubin, M.; Bremer, C.; Ollivier, J.; de Meijere, A.; Saulün, J. Diastereoselective palladium(0)-catalyzed azidation of 1-alkenylcyclopropyl esters: asymmetric synthesis of (–)-(1*R*,2*S*)-norcoronamic acid. *Tetrahedron Asymmetry* **1998**, 1131–1135; (f) Martin, S. F.; Dwyer, M. P. Iodocyclopropanes as versatile intermediates for the synthesis of substituted cyclopropanes. *Tetrahedron Lett.* **1998**, *39*, 1521–1524; (g) Luithle, J. E. A.; Pietruszka, J. (2*R*,3*R*)-1,4-Dimethoxy-1,1,4,4-tetraphenyl-2,3-butanediol: Chiral Auxiliary and Efficient Protecting Group for Boronic Acids. *J. Org. Chem.* **2000**, *65*, 9194–9200; (h) Hohn, E.; Pietruszka, J. Enantiomerically Pure Cyclopropane Building Blocks: Synthesis and Transformations of 2-Iodocyclopropylboronic Esters. *Adv. Synth. Catal.* **2004**, *346*, 863–866; (i) Wu, X.; Lecornué, F.; Charnay-Pouget, F.; Ollivier, J. π-Allyl Palladium Complexes as Efficient and Powerful Alternative for Nucleophilic Substitution on Bicyclo[3.1.0]hexane Sulfonates: Regio-, Chemo- and Stereoselectivity. *Synlett* **2006**, 1407–1409; (j) Lei, C.; Yue, G.; Zhou, J. Palladium-Catalyzed Direct Cyclopropylation of Heterocycles. *Angew. Chem. Int. Ed.* **2015**, *54*, 9601–9605; (k) Allouche, E. M. D.; Taillemaud, S.; Charette, A. B. Spectroscopic characterization of (diiodomethyl)zinc iodide: application to the stereoselective synthesis and functionalization of iodocyclopropanes. *Chem. Commun.* **2017**, *53*, 9606–9609.

19. Pioneering references: (a) Kulinkovich, O. G.; Sviridov, S. V.; Vasilevskii, D. A.; Prityts kaya, T. S. Reaction of ethylmagnesium bromide with carboxylic esters in the presence of tetraisopropoxytitanium. *Zh. Org. Chem.* **1989**, *25*, 2244–2245; (b) Kulinkovich, O. G.; Sviridov, S. V.; Vasilevski, D. A. Titanium(IV) Isopropoxide-Catalyzed Formation of 1-Substituted Cyclopropanols in the Reaction of Ethylmagnesium Bromide with Methyl Alkanecarboxylates. *Synthesis*, **1991**, 234–234; Reviews: (c) Kulinkovich, O. G. The Chemistry of Cyclopropanols. *Chem. Rev.* **2003**, *103*, 2597–2632; (d) Mills, L. R.; Rousseaux, S. A. L. Modern Developments in the Chemistry of Homoenolates. *Eur. J. Org. Chem.* **2019**, 8–26.

20. Talele, T. T. The "Cyclopropyl Fragment" is a Versatile Player that Frequently Appears in Preclinical/Clinical Drug Molecules. *J. Med. Chem.* **2016**, *59*, 8712–8756.

21. Wu, W.; Lin, Z.; Jiang, H. Recent advances in the synthesis of cyclopropanes. *Org. Biomol. Chem.* **2018**, *16*, 7315–7329.

22. (a) Faul, M. M.; Ratz, A. M.; Sullivan, K. A.; Trankle, W. G.; Winneroski, L. L. *J. Org. Chem.* **2001**, *66*, 5772–5782; (b) Kuk, K.; Taylor-Cousar, J. L. *Ther. Adv. Respir. Dis.* **2015**, *9*, 313–326.

23. McCann, L. C.; Organ, M. G. On The Remarkably Different Role of Salt in the Cross-Coupling of Arylzincs From That Seen With Alkylzincs. *Angew. Chem. Int. Ed.* **2014**, *53*, 4386–4389 and references cited therein.
24. It is currently unknown what the mechanism of formation for this product is, though we believe S_N2'-type and S_N1-type mechanisms are likely possibilities.
25. (a) Lackner, G. L.; Quasdorf, K. W.; Overman, L. E. Direct Construction of Quaternary Carbons from Tertiary Alcohols via Photoredox-Catalyzed Fragmentation of *tert*-Alkyl *N*-Phthalimidoyl Oxalates. *J. Am. Chem. Soc.* **2013**, *135*, 15342–15345; (b) Pratsch, G.; Lackner, G. L.; Overman, L. E. Constructing Quaternary Carbons from *N*-(Acyloxy)phthalimide Precursors of Tertiary Radicals Using Visible-Light Photocatalysis. *J. Org. Chem.* **2015**, *80*, 6025–6036.
26. (a) Barton, D. H. R.; McCombie, S. W. A New Method for the Deoxygenation of Secondary Alcohols. *J. Chem. Soc., Perkin Trans. 1* **1975**, 1574–1585; (b) McCombie, S. W.; Quiclet-Sire, B.; Zard, S. Z. Reflections on the mechanism of the Barton-McCombie Deoxygenation and on its consequences. *Tetrahedron* **2018**, *74*, 4969–4979; (c) Lopez, R. M.; Hays, D. S.; Fu, G. C. Bu_3SnH-Catalyzed Barton–McCombie Deoxygenation of Alcohols. *J. Am. Chem. Soc.* **1997**, *119*, 6949–6950.
27. (a) Bachi, M. D.; Bosch, E. Synthesis of α-alkylidene-γ-lactones by intramolecular addition of alkoxycarbonyl free-radicals to acetylenes. *Tetrahedron Lett.* **1986**, *27*, 641–644; (b) Nozaki, K.; Oshima, K.; Utimoto, K. Synthesis of lactones by intramolecular addition of alkoxythiocarbonyl free radicals to acetylenes. *Tetrahedron Lett.* **1988**, *29*, 6127–6128; (c) Angoh, A. G.; Clive, D. L. J. Radical annulation: a method for preparation of carbocycles. *J. Chem. Soc., Chem. Commun.* **1985**, 980–982; (d) Yamamoto, M.; Uruma, T.; Iwasa, S.; Kohmoto, S.; Tamada, K. Tri-*n*-butyltin hydride assisted highly stereoselective lactonisation of homoallylic xanthates. *J. Chem. Soc., Chem. Commun.* **1989**, 1265–1267; (e) Bachi, M. D.; Bosch, E. Free Radical Cyclization of Thionocarbonic Acid Derivatives of 4-Phenyl-3-butenol. A New Route to Thionolactones. *J. Org. Chem.* **1989**, *54*, 1234–1236; (f) Iwasa, S.; Yamamoto, M.; Kohmoto, S.; Yamada, K. Synthesis of thionolactones from homoallylic xanthates. *J. Chem. Soc., Perkin Trans. 1* **1991**, 1173–1176; (g) Iwasa, S.; Yamamoto, M.; Kohmoto, S.; Yamada, K. Tandem radical cyclization of acyclic homoallylic xanthates: cyclopentannulated γ-thionolactone and γ-lactones. *J. Org. Chem.* **1991**, *56*, 2849–2853; (h) Bachi, M. D.; Bosch, E.; Denenmark, D.; Girsh, D. Tributylstannane-mediated cyclization of thionocarboxylic acid derivatives. *J. Org. Chem.* **1992**, *57*, 6803–6810; (i) Coote, M. L.; Easton, C. J.; Zard, S. Z. Factors Affecting the Relative and Absolute Rates of β-Scission of Alkoxythiocarbonyl Radicals and Alkoxycarbonyl Radicals. *J. Org. Chem.* **2006**, *71*, 4996–4999; (j) Alberti, A.; Bengalia, M.; Guerra, M.; Gulea, M.; Macciantelli, D.; Masson, S. On the Actual EPR Detection of Thioacyl Radicals. *Org. Lett.* **2008**, *10*, 3327–3330; (k) Davy, J. A.; Mason, J. W.; Moreau, B.; Wulff, J. E. Xanthates as Synthetic Equivalents of Oxyacyl Radicals: Access to Lactones under Tin-Free Conditions. *J. Org. Chem.* **2012**, *77*, 6332–6339.
28. We think a 2e oxidative addition mechanism into the acyl C–N bond is unlikely, since conversion of **1k** to **4** shows a strong ligand dependence, with ligands that are typically good for acyl C–N oxidative addition being poor for this process (see Table S2); (a) Hie, L.; Fine Nathel, N. F.; Shah, T. K.; Baker, E. L.; Hong, X.; Yang, Y.-F.; Liu, P.; Houk, K. N.; Garg, N. K. Conversion of amides to esters by the nickel-catalysed activation of amide C–N bonds. *Nature* **2015**, *524*, 79–83; (b) Shi, S.; Szostak, M. Efficient Synthesis of Diaryl Ketones by Nickel-Catalyzed Negishi Cross-Coupling of Amides by Carbon–Nitrogen Bond Cleavage at Room Temperature Accelerated by a Solvent Effect. *Chem. Eur. J.* **2016**, *22*, 10420–10424.
29. Standard conditions match those shown in Table 2, using ArZnOMe (3 equiv), $Ni(acac)_2 \bullet xH_2O$ (10 mol %), bathocuproine (20 mol %), and $MgCl_2$ (2 equiv), in 1,4-dioxane/THF (3:1) at 23 ºC for 12 h. See SI (Table S11) for details.
30. This sample also contained 4,4'-difluoro-1,1'-biphenyl, which was inseparable from the desired product.
31. Alabugin, I. V.; Gomes, G. P.; Abdo, M. ref: I. V. Alabugin, G. P. Gomes, M. Abdo. Hyperconjugation. *WIREs Comput. Mol Sci.* **2018**, *9*, e1389.
32. Computed with NBO7 interfaced to Gaussian '16. NBO 7.0 can be obtained at: http://nbo7.chem.wisc.edu. Glendening, E. D.; Landis, C. R.; Weinhold, F. NBO 7.0: New vistas in localized and delocalized chemical bonding theory. *J. Comput. Chem.* **2019**, *40*, 2234–2241.
33. Vatsadze, S. Z.; Loginova, Y. D.; Gomes, G. P. Alabugin, I. V. Stereoelectronic Chameleons: The Donor–Acceptor Dichotomy of Functional Groups *Chem. Eur. J.* **2017**, *23*, 3225–3245.
34. The chameleonic behavior of σ-acceptors involved in the selective TS-stabilization of negative charges has been demonstrated on: (a) the synthesis of poly(aryl thioesteres): Park, N. H.; Gomes, G. P.; Fevre, M.; Jones, G. O.; Alabugin, I. V.; Hedrick, J. L. Organocatalyzed Synthesis of Fluorinated Poly(aryl thioethers). *Nat. Commun.* **2017**, *8*, 166, doi: 10.1038/s41467-017-00186-3. (b) the cyclization of enediynes Peterson, P.; Shevchenko, N.; Breiner, B.; Manoharan, M.; Lufti, F.; Delaune, J.; Kingsley, M.; Kovnir, K.; Alabugin, I. V. Orbital Crossings Activated Through Electron Injection: Opening Communication between Orthogonal Orbitals in Anionic C1-C5 Cyclizations of Enediynes. *J. Am. Chem. Soc.,* **2016***, 138,* 15617
35. The corresponding thioester was also obtained in 12% isolated yield. Other side-products include vinylnaphthalene, resulting from β-hydride elimination prior to reductive elimination, which was present in 1% yield by ^1H NMR, and 4-methoxybenzophenone and 4,4'-dimethoxybenzophenone, whose yields weren't determined.
36. Walborsky, H. M.; Chen, C.-J. Cyclopropanes. XXIX. The Stereochemistry of the 1-Methyl-2,2-diphenylcyclopropyl Radical in and out of Solvent Cage. *J. Am. Chem. Soc.* **1971**, *93*, 671–675.
37. (a) Walborsky, H. M.; Allen, L. E. The Stereochemistry of Tris(triphenylphosphine)rhodium Chloride Decarbonylation of Aldehydes. *J. Am. Chem. Soc.* **1971**, *93*, 5465–5468; (b) Miura, T.; Makamura, T.; Stewart, S. G.; Nagata, Y.; Murakami, M. Synthesis of Enantiopure C_3-

Symmetric Triangular Molecules. *Angew. Chem. Int. Ed.* **2017**, *56*, 3334–3338.

38. Short-lived non-cyclopropyl radical intermediates can also maintain stereochemistry: (a) Bartlett, P. D.; McBride, J. M. Configuration, conformation and spin in radical pairs. *Pure Appl. Chem.* **1967**, *15*, 89–108; (b) Kopecky, K. R.; Gillan, T. Thermal decomposition of optically active unsymmetrical azoalkanes. (–)-(*S*)-1,1'-Diphenyl-1-methylazomethane. *Can. J. Chem.* **1969**, *47*, 2371–2386; (c) Greene, F. D.; Berwick, M. A.; Stowell, J. C. Stereochemistry of Free-Radical Recombination Reactions. Cage effect in decomposition of *SS*-(–)-Azobis-α-phenylethane. *J. Am. Chem. Soc.* **1970**, *92*, 867–874.

39. The rate of inversion for 1-methylcyclopropyl radical is 2.1×10^8 s^{-1}, and the barrier to inversion increases with substituent size. In comparison, rate of diffusion from the solvent cage is much faster, estimated at 10^{11} s^{-1}: (a) Johnston, L. J.; Ingold, K. U. Kinetics of cyclopropyl radical reactions. 2. Studies on the inversion of cyclopropyl and 1-methylcyclopropyl radicals and on the kinetics of some addition and abstraction reactions of 1-methylcyclopropyl and 1-methoxycyclopropyl radicals. *J. Am. Chem. Soc.* **1986**, *108*, 2343–2348; (b) S. W. Benson, Foundations of Chemical Kinetics. McGraw-Hill, New York, **1960**.

40. We estimate that the rate of in-cage radical rebound would be faster than the rate of diffusion, which is therefore faster than the rate of inversion for the cyclopropyl radical. At this rate of radical recombination, other radical clocks would not be informative. The rate of ring-opening of cyclopropylcarbinyl radical is 1.3×10^8 s^{-1}, and the rate of $C(sp^3)$ radical *5-exo-trig* cyclization is 1.0×10^5 s^{-1}, which is slower for benzylic $C(sp^3)$ radicals: (a) Griller, D.; Ingold, K. U. Free-radical clocks. *Acc. Chem. Res.* **1980**, *13*, 317–323; (b) Radical Reactions in Organic Synthesis. Zard, S. Z. Oxford: Oxford University Press, **2003**.

41. Performing the standard reaction in the presence of 1 equiv of a radical trap like styrene or benzyl acrylate resulted in no detectable formation of a radical adduct, consistent with radical intermediates not escaping the solvent cage (Table S10). Performing the reaction in the presence of 1 equiv TEMPO shut down the reaction.

42. As an additive, $MgCl_2$ (2 equiv) was empirically found to help with reproducibility across batches of arylzinc reagent, since zinc(II) halides promoted cleavage of the *N*–benzoyl group to form 4-methoxybenzophenone, and which side-reaction could be slightly retarded with the addition of $MgCl_2$ (cf. Table S3, entries 9 and 14).

43. The major side-products in this reaction are the ketone resulting from oxidative addition of the *N*–Bz bond, the ketone resulting from double addition into the carbamate followed by hydrolysis, as well as thioester **4** (see optimization tables in SI for side-product yields).

44. *Gaussian '16*, Revision C.01, full reference in the ESI.

45. (a) O'Boyle, N. M.; Banck, M.; James, C. A.; Morley, C.; Vandermeersch, T.; Hutchison, G. R. Open Babel: An open chemical toolbox. *J. Cheminf.*, **2011**, *3*, 33; (b) The Open Babel Package, version 2.3.1 http://openbabel.org (accessed Feb. 2019).

46. *xtb* can be freely obtained at**:** https://github.com/grimme-lab/xtb; Bannwarth, C.; Ehlert, S.; Grimme, S. GFN2-xTB—An Accurate and Broadly Parametrized Self-Consistent Tight-Binding Quantum Chemical Method with Multipole Electrostatics and Density-Dependent Dispersion Contributions. *J. Chem. Theory Comput.* **2019**, *15*, 1652–1671.

47. Grimme, S. Exploration of Chemical Compound, Conformer, and Reaction Space with Meta-Dynamics Simulations Based on Tight-Binding Quantum Chemical Calculations. *J. Chem. Theory Comput.* **2019**, *15*, 2847–2862.

48. Marenich, A. V.; Cramer, C. J.; Truhlar, D. G. Universal solvation model based on solute electron density and a continuum model of the solvent defined by the bulk dielectric constant and atomic surface tensions. *J. Phys. Chem. B*, **2009**, *113*, 6378–6396.

49. Chai, J.-D.; Head-Gordon, M. Long-range corrected hybrid density functionals with damped atom-atom dispersion corrections. *Phys. Chem. Chem. Phys.*, **2008**, *10*, 6615–6620.

50. (a) Grimme, S.; Antony, J.; Ehrlich, S.; Krieg, H. A consistent and accurate *ab initio* parametrization of density functional dispersion correction (DFT-D) for the 94 elements H–Pu. *J. Chem. Phys.,* **2010**, *132*, 154104–154119; (b) Grimme, S.; Ehrlich, S.; Goerigk, L. Effect of the damping function in dispersion corrected density functional theory. *J. Comp. Chem.*, **2011**, *32*, 1456–1465.

51. *GoodVibes* can be freely obtained at: https://github.com/bobbypaton/GoodVibes; Luchini, G.; Alegre-Requena, J. V.; Funes-Ardoiz, I.; Paton, R. S. GoodVibes: Automated Thermochemistry for Heterogeneous Computational Chemistry Data. *F1000Research*, **2020**, *9*, 291.

52. (a) Weinhold, F.; Landis, C. R.; Glendening, E. D. What is NBO analysis and how is it useful? *Int. Rev. Phys. Chem.* **2016**, *35*, 399–440; (b) Reed, A. E.; Weinhold, F. Natural localized molecular orbitals. *J. Chem. Phys.,* **1985**, *83*, 1736–1740; (c) Reed, A. E.; Weinhold, F. Natural Bond Orbital Analysis of Internal Rotation Barriers and Related Phenomena. *Isr. J. Chem.*, **1991**, *31*, 277–285; (d) Reed, A. E.; Curtiss, L. A.; Weinhold, F. Intermolecular interactions from a natural bond orbital, donor-acceptor viewpoint. *Chem. Rev.,* **1988**, *88*, 899–926; (e) Weinhold F. Natural Bond Orbital Methods. In Schleyer. P.v.R., *Encyclopedia of Computational Chemistry*: Wiley: New-York, **1998**, *3*, 1792.

53. CYLview, 1.0b; Legault, C. Y., Université de Sherbrooke, 2009 (http://www.cylview.org).

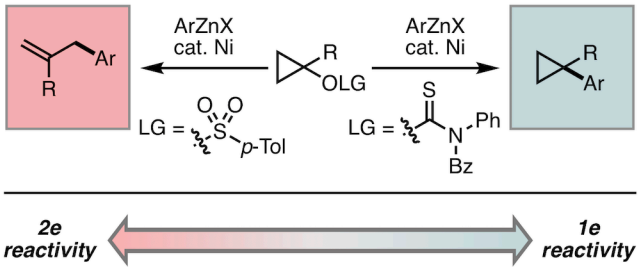
ArZnX
cat. Ni
R
OLG
ArZnX
cat. Ni
Ar
R
LG =
O
O
S
p-Tol
LG =
S
N
Ph
Bz
R
Ar
2e
reactivity
1e
reactivity

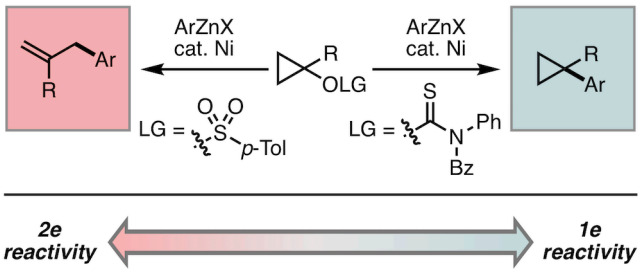
ArZnX
cat. Ni
ArZnX
cat. Ni
Ar
R
R
OLG
R
Ar
LG =
p-Tol
LG =
Ph
Bz
2e
reactivity
1e
reactivity